

A COMPARISON OF COMPUTATIONAL METHODS TO DETERMINE THE PERMEABILITY OF VERTEBRAL TRABECULAR BONE

¹René P. Widmer and ¹Stephen J. Ferguson

¹Institute for Surgical Technology and Biomechanics, University of Bern, Bern, Switzerland,
email: rene.widmer@istb.unibe.ch, web: www.istb.unibe.ch

INTRODUCTION

As the carrier of a homogeneous fluid in viscous motion, a uniform porous medium may be completely described by the specification of its permeability. The term permeability may be defined physically as the volume of a fluid of unit viscosity passing through, in unit time, a unit cross-section of the porous medium under the influence of a unit pressure gradient, or, as the macroscopic velocity of a particle of a unit viscosity fluid at a point in the medium at which the pressure gradient is unity. Defined in this way, the permeability of a porous medium, e.g. trabecular bone, generally is independent of the absolute pressure or velocities within the flow system, or of the nature of the fluid, and is characterized only by the structure of the medium. Fluid flow in the intertrabecular spaces has been implicated in a number of physiological phenomena. For example, flow induced shearing stresses play a key role in regulating bone metabolism. In relation to the augmentation of osteoporotic bone, it has been hypothesized that the ability of polymethylmetacrylate to flow into the trabecular bone affects the spreading pattern of the bone cement and consequently the mechanical outcome of the bone augmentation.

Recently, several studies extensively investigated the dependence of intrinsic permeability on trabecular bone morphology and anatomical direction either experimentally [1,2,3] or computationally [4,5]. This study addresses the comparison of four computational methods including a characterization of the prediction error related to each method individually. The investigated methods use input data acquired on length scales varying from tissue to organ level, thus we also determine and quantify the amount of information that is required to accurately predict intrinsic bone permeability.

METHODS

Microscale simulations of a Newtonian flowing through the cavities of 3 aluminum foam samples (m.Pore GmbH, Dresden) that simulate the microstructure of vertebral trabecular bone were reconstructed from microCT scans at a resolution of 20 μ m. Each sample had dimensions of 2x2x2 mm³. The image stacks were morphologically manipulated (erosion, dilatation) to mimic the effect of varying structural porosity. The creeping flow regime ($Re \ll 1$) has been governed by the steady-state Stokes equation

$$\nabla p - \mu \nabla^2 \mathbf{u} = 0. \quad (1)$$

p refers to the fluid pressure gradient, μ to the viscosity and \mathbf{u} to the fluid velocity vector. This equation has been numerically solved using the Finite Element method (Figure 1) by implementing the residual form of Eq. (1) into the open source FE library *libMesh*.

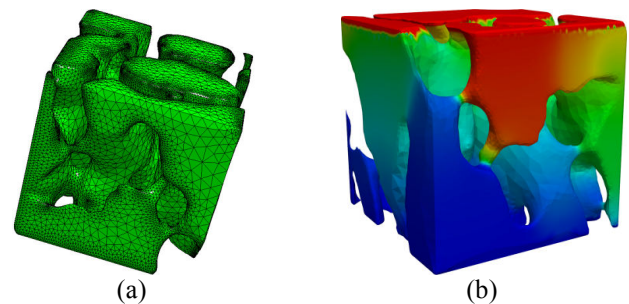


Figure 1: Tetrahedral mesh (a) and computed pressure field (b) of Newtonian and creeping flow through a representative aluminum foam sample

On the same length scale, permeability values have also been computed using a pore network modeling algorithm (Figure 2). From the micro-architecture, an aperture map representing the local pore radii has been derived. Pore boundaries are determined utilizing a watershed transformation and segmentation. Both aperture and pore boundary map provide information for a pore network to approximate the flow channels of the porous structure.

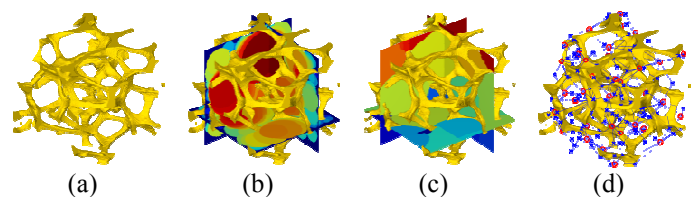


Figure 2: The aperture map (b), the pore map (c) and the pore network model are derived from a microCT image stack (a) of aluminum foams to estimate its intrinsic permeability

Each link in the pore network is represented by a conical pipe to express the hydraulic conductivity g_{ij} as a function of the link length and the pore radii. The local flow rates $q = \frac{Q}{A}$ are found by solving the equation system $\mathbf{P} = \mathbf{g} \cdot \mathbf{Q}$. For both the FE and pore network approach, permeability values are derived by averaging the fluid flow velocities over the inlet and/or outlet area A and insertion into the rearranged Darcy equation, thus

$$k^S = \frac{\mu q}{\nabla p}. \quad (2)$$

k^S represents the intrinsic permeability and q the flow rate. We pre-computed permeability values using an analytical model ([6], Figure 3) of vertebral trabecular bone accepting morphological information (porosity, trabecular spacing, degree of anisotropy) as model input. The pre-computed values were analyzed using a log-linear regression analysis [5], thus permeability can be estimated from mesoscale morphology data according to

$$\log_{10}(k^S) = \alpha_0 + \alpha_1\beta + \alpha_2DA + \alpha_3Tb.Sp^{(h)} + \alpha_4Tb.Sp^{(v)}, \quad (3)$$

where β refers to the porosity, DA to the degree of anisotropy and $Tb.Sp^{(h/v)}$ to the horizontal and vertical spacing of the trabecular bone. Horizontal and vertical spacing values have been extracted utilizing an in house skeletonization and triangulation algorithm from the subsequently down sampled microCT scans and the degree of anisotropy is given by

$$DA = \frac{Tb.Sp^{(v)}}{Tb.Sp^{(h)}}.$$

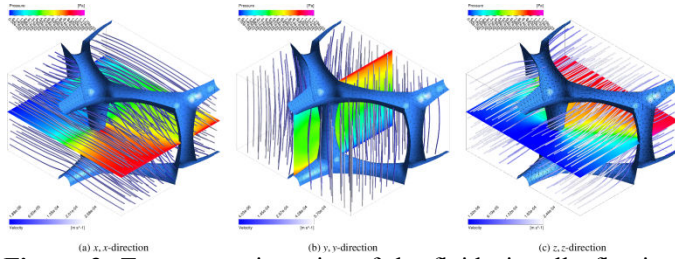


Figure 3: Tortuous trajectories of the fluid virtually flowing through the analytical unit cell used to pre-compute permeability values of vertebral trabecular bone

On the macroscopic length scale, only the bone volume ratio can be evidently estimated. Consequently, the presented regression model reduces to $\log_{10}(k^S) = \alpha_0 + \alpha_1\beta$. Baroud et al. [1] independently provide a similar regression model in the form of $k_{ij}^S = \Gamma_{ij} \frac{\beta}{1-\beta}$, where Γ_{ij} represents the fitting coefficient of the ij -th direction and has also been included into the benchmarking of this study.

RESULTS AND DISCUSSION

Morphometry indicated trabecular spacing of {1.0976, 0.8441, 1.0250} mm (horizontal) and {1.5234, 1.1919, 1.4310} mm (vertical) and anisotropy degrees of {1.3880, 1.4120, 1.3960}, respectively. The permeability values as a function of structural porosity are shown in Figure 4. Circle markers in the plot refer to experimental data from literature. Crossed markers represent results computationally determined on a microscopic length scale either using the pore network model or the Stokes flow code. The lines show the responses over the investigated porosity range (macroscale model) or the porosity range related to each foam sample (mesoscale model). The colored area expresses (un)certainty, i.e. probabilistic density, induced by partially ignoring morphological information

(thickness, trabecular and joint shape). At small porosity values, and thus compact porous structure, thickness and trabecular shape are of minor relevance and consequently certainty is high. For very porous bone, permeability is not only a function of porosity and certainty is low. Transversal direction: the computational methods consistently agree with each other and lie in the range of the experimental values from literature. Longitudinal direction: permeability values of the regression model are located at the upper range of the experimental values and the analytical model indicates a higher uncertainty compared to the transversal direction. Microscale simulation results are significantly lower. An explanation to that could be the more isotropic structure of the foams compared to that of vertebral trabecular bone. Thus permeability does not much differ among the different directions.

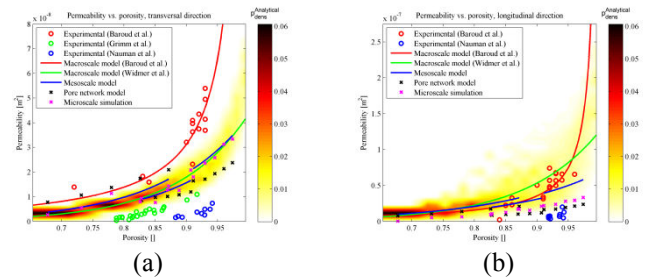


Figure 4: Various experimental and computed permeability values of vertebral trabecular bone and aluminum foam

CONCLUSIONS

We have presented different methods to estimate the permeability of aluminum foam, and potentially vertebral trabecular bone, that are based on digitized datasets acquired on different length scale levels and consequently provide generally consistent results, however with a varying prediction accuracy. At the moment, our estimation trials were conducted based on aluminum foam samples that do not perfectly match the micro-architecture of vertebral trabecular bone. Effort is ongoing by collecting and scanning representative human bone samples. Based on that data, a more conclusive statement regarding the accuracy of each individual method can be given.

ACKNOWLEDGEMENTS

Funding for this research project was provided by the European Union (project FP7-ICT-223865-VPHOP). The authors also would like to express their gratitude to ANSYS for providing CFX under a university research license.

REFERENCES

1. Baroud G, et al. *J. Biomech.* **37**:189-196, 2004.
2. Nauman EA, et al., *Ann. Biomed. Eng.* **27**:517-524, 1999.
3. Grimm MJ, et al., *J. Biomech.* **30**:743-745, 1997.
4. Zeiser T, et al., *Proc Inst Mech Eng [H]* **222**:185-194.
5. Widmer RP, et al., *J. Bone*. In review.
6. Kim HS, et al., *J. Biomech.* **35**:1101-1114, 2002